



Swansea University
Prifysgol Abertawe



Cronfa - Swansea University Open Access Repository

This is an author produced version of a paper published in:
Developmental & Comparative Immunology

Cronfa URL for this paper:
<http://cronfa.swan.ac.uk/Record/cronfa39536>

Paper:

Coates, C. & Talbot, J. (2018). Hemocyanin-derived phenoloxidase reaction products display anti-infective properties.
Developmental & Comparative Immunology
<http://dx.doi.org/10.1016/j.dci.2018.04.017>

12 month embargo.

This item is brought to you by Swansea University. Any person downloading material is agreeing to abide by the terms of the repository licence. Copies of full text items may be used or reproduced in any format or medium, without prior permission for personal research or study, educational or non-commercial purposes only. The copyright for any work remains with the original author unless otherwise specified. The full-text must not be sold in any format or medium without the formal permission of the copyright holder.

Permission for multiple reproductions should be obtained from the original author.

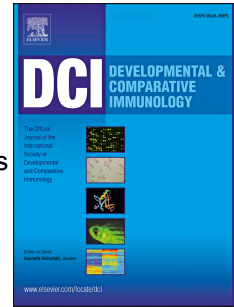
Authors are personally responsible for adhering to copyright and publisher restrictions when uploading content to the repository.

<http://www.swansea.ac.uk/library/researchsupport/ris-support/>

Accepted Manuscript

Hemocyanin-derived phenoloxidase reaction products display anti-infective properties

Christopher J. Coates, James Talbot



PII: S0145-305X(18)30166-6

DOI: [10.1016/j.dci.2018.04.017](https://doi.org/10.1016/j.dci.2018.04.017)

Reference: DCI 3153

To appear in: *Developmental and Comparative Immunology*

Received Date: 2 April 2018

Revised Date: 20 April 2018

Accepted Date: 21 April 2018

Please cite this article as: Coates, C.J., Talbot, J., Hemocyanin-derived phenoloxidase reaction products display anti-infective properties, *Developmental and Comparative Immunology* (2018), doi: 10.1016/j.dci.2018.04.017.

This is a PDF file of an unedited manuscript that has been accepted for publication. As a service to our customers we are providing this early version of the manuscript. The manuscript will undergo copyediting, typesetting, and review of the resulting proof before it is published in its final form. Please note that during the production process errors may be discovered which could affect the content, and all legal disclaimers that apply to the journal pertain.

Abstract

Hemocyanin is a multi-functional protein located in the hemolymph (blood) of certain arthropods and molluscs. In addition to its well-defined role in oxygen transport, hemocyanin can be converted into a phenoloxidase-like enzyme. Herein, we tested the antimicrobial properties of horseshoe crab (*Limulus polyphemus*) hemocyanin-derived phenoloxidase reaction products using broad ranges of phenolic substrates (e.g. L-DOPA) and microbial targets (Gram-positive/negative bacteria, yeast). The enzyme-catalysed turnover of several substrates generated (by)products that reduced significantly the number of colony forming units. Microbicidal effects of hemocyanin-derived phenoloxidase were thwarted by the inhibitor phenylthiourea. Data presented here further support a role for hemocyanin in invertebrate innate immunity.

Keywords:

Horseshoe crabs; Innate immunity; Melanogenesis; Enzyme-substrate complexes; Multifunctional protein

1. Introduction

Broadly, invertebrate innate immunity is an assemblage of physical barriers, cellular defences coordinated by hemocytes, and diverse humoral (soluble) factors within the hemolymph. One of the most effective invertebrate responses to disease-causing agents – microbes or parasites – is the production of melanin via the pro-phenoloxidase (proPO) cascade (Cerenius *et al.*, 2008). Activated phenoloxidases (POs) convert mono/di-phenolic substrates into reactive quinones, which are further processed enzymatically/non-enzymatically into 5,6-dihydroxyindoles (DHI) and eventually eumelanin. Melanic polymers and toxic by-products of PO-associated

to possess a true PO, instead they rely on the inducible enzyme activity of another type-3 copper protein, namely hemocyanin (Baird *et al.*, 2007; Schenk *et al.*, 2015). Hemocyanin (Hc), the invertebrate oxygen-transport protein, is a versatile immune effector displaying virustatic properties and acting as a precursor of antimicrobial peptides (AMPs) in arthropods and molluscs (Lee *et al.*, 2003; Dolashka *et al.*, 2016; Coates and Decker, 2017). The dicopper active sites of Hc and PO are structurally conserved – consisting of an α -helical (tyrosinase) domain wherein six invariant copper-coordinating histidine residues facilitate the binding of dioxygen between CuA and CuB. Horseshoe crab Hc can be converted into a PO-like enzyme *in vivo* when exposed to clotting factors (Nagai and Kawabata, 2000), antimicrobial peptides (Nagai *et al.*, 2001), proteases (Jiang *et al.*, 2007), or inner membrane phospholipids (Coates *et al.*, 2011; 2013). It remains unclear whether hemocyanin-derived phenoloxidase (Hc-d PO) activities are directly antimicrobial. Therefore, we set out to explore the enzymatic role of activated Hc in horseshoe crab (*Limulus polyphemus*) innate immunity. This was achieved by [1] characterising Hc-substrate kinetics in the presence of common diphenols, and [2] monitoring the growth of microbes exposed to the respective Hc-catalysed products.

2. Materials and methods

2.1 Hemocyanin-derived phenoloxidase assays

Hemocyanin (Hc) was purified from horseshoe crabs (*L. polyphemus*) following the protocol of Coates *et al.* (2011; 2013). Briefly, hemolymph was extracted from the cardiac sinus using a hypodermic needle and centrifuged (500x *g* 5 min, 4°C) to remove the cellular fraction. The supernatant was ultra-centrifuged (300,000x *g*, 90 min, 4°C) and the protein pellet was re-suspended in stabilisation buffer (100 mM Tris-HCl pH7.5, 5 mM CaCl₂, 5 mM MgCl₂) before being applied to a pre-calibrated size-exclusion column (Sephacryl S-500 HR).

Spectrophotometric measurements of enzyme activity were performed at 20°C using either a V-1200 spectrophotometer (VWR) or a SpectroStar Nano (equipped with a cuvette port and microplate reader). Typically, assays consisted of 100 mM Tris-HCl, pH 7.5, 1 mgmL⁻¹ purified hemocyanin and 0.1% SDS (3.5 mM). Hemocyanin was incubated in the presence of the anionic detergent SDS for 5 minutes (20°C) to activate the protein prior to the addition of substrates across several concentration ranges: catechol (0 – 100 mM), dopamine hydrochloride (0 – 5 mM), 3,4-Dihydroxycinnamic acid (caffeic acid; 0 – 5 mM), 3,4-Dihydroxyphenylacetic acid (DOPAC; 0 – 5 mM), 3,4-Dihydroxy-L-phenylalanine (L-DOPA; 0 – 5 mM), 4-Methylcatechol (4-MC; 0 – 30 mM), 4-Methylphenol (5 mM), 4-Methoxyphenol (5 mM), L-tyrosine (5 mM), and 4-*tert*-Butylcatechol (4-TBC; 0 – 5 mM). Assays were run for 5-10 minutes. An increase in absorbance at 475 nm is indicative of product formation. Enzyme activity was converted to μ mol dopachrome formed per minute

2.2 Microbial targets – culturing and preparation

Gram-negative bacteria (*Escherichia coli* strain M15, *Pantoea agglomerans* (formerly *Erwinia herbicola*)), Gram-positive bacteria (*Bacillus megaterium*, *Bacillus subtilis*, *Micrococcus luteus*), and the yeast *Saccharomyces cerevisiae* strain AH22 were used as microbial targets. Single colonies of bacteria and yeast were selected from nutrient agar (Thermo Scientific Oxoid) and YEPD (1% [w/v] yeast extract, 2% [w/v] Bacto peptone, 2% [w/v] D-glucose, 2% [w/v] agar), respectively, and cultured overnight in broth – 37°C for bacteria (except *P. agglomerans*) and 30°C for yeast. After reaching an OD₆₀₀ value of 1, 1 mL of each microbial culture was centrifuged at 1000 x g for 5 minutes at room temperature and washed twice in buffer (100 mM Tris-HCl, pH 7.5). Microbial suspensions were diluted in buffer to achieve 1 x10⁶ colony forming units (CFUs) per mL.

2.3 Antimicrobial activity of hemocyanin-catalysed reaction products

Upon completion of hemocyanin-derived phenoloxidase (Hc-d PO) assays using 2 mM of selected substrates (dopamine, L-DOPA, 4-MC or 4-TBC), the reaction mixtures (1 mL) were centrifuged at 4,000 x g for 5 minutes at room temperature using Amicon Ultra Filter Units (Millipore) with a 10 kDa cut-off to remove the hemocyanin (~70 kDa per subunit). Microbial suspensions (100 uL) were mixed with an equal volume of enzyme reaction products (i.e. filtrates) and incubated at room temperature for 1 hour. Once complete, the mixtures were serially diluted in 100 mM Tris-HCl, pH 7.5 so that ~200 CFUs were spread across nutrient or YEPD media (2% [w/v] agar). Inoculated plates were incubated for up to 48 hours at either 30°C (*S. cerevisiae*, *P. agglomerans*) or 37°C (remaining bacteria) prior to colony counting. In order to attribute the observed antimicrobial activity to hemocyanin-derived phenoloxidase reaction products alone, Hc (1 mgmL⁻¹) was exposed to the highly specific phenoloxidase inhibitor phenylthiourea (10 µM) alongside SDS (as stated above) prior to the addition of substrate.

2.4 Data handling

Enzyme assays for hemocyanin-derived phenoloxidase were performed on three independent occasions. Data were processed using Michaelis-Menten (non-linear regression) kinetics or Lineweaver-Burk plots for K_M, V_{max}, and K_{cat} calculations. Antimicrobial assays were performed on three independent occasions in duplicate (two technical replicates) with data subjected to ANOVA and Tukey's multiple comparisons tests. Differences were considered significant at $P \leq 0.05$. GraphPad PRISM v7 was used to prepare figures and perform statistical analyses.

Horseshoe crab Hc was activated successfully using SDS and assessed for substrate preference across 7 diphenols and 3 monophenols. No measureable monophenolase activity was recorded for Hc presented with 5 mM of either 4-methoxyphenol, 4-methylphenol or L-tyrosine under our experimental conditions. Conversely, Hc was capable of oxidising all *ortho*-diphenols into their corresponding *ortho*-quinones (Table 1). At concentrations ≤ 5 mM for L-DOPA, dopamine and 4-TBC, and ≤ 30 mM for 4-MC, kinetic data were interrogated using the Michaelis-Menten equation. Goodness of fit values ranged from ~ 0.95 to 0.98 for non-linear regression (Figure 1). The Michaelis-Menten constant (K_M) for dopamine was revealed to be the lowest at ~ 0.8 mM, suggesting that it is the preferred substrate. This was followed by a K_M value of ~ 1.2 mM for 4-TBC. Maximum velocity (V_{max}) ranged from ~ 1.3 $\mu\text{mol min}^{-1}$ for DOPAC to 9.3 $\mu\text{mol min}^{-1}$ for 4-TBC (Table 1). Catalytic efficiency (K_{cat}/K_M) for Hc-d PO varied considerably from 0.12 $\text{mM}^{-1} \text{S}^{-1}$ for DOPAC to 5.71 $\text{mM}^{-1} \text{S}^{-1}$ for 4-TBC. When comparing the catalytic efficiency of the two most physiologically relevant diphenols for invertebrate melanogenesis, dopamine (4.4 $\text{mM}^{-1} \text{S}^{-1}$) was over seven-fold higher than its precursor L-DOPA (~ 0.6 $\text{mM}^{-1} \text{S}^{-1}$) (Table 1). Similarly, Jaenicke and Decker (2008) calculated catalytic efficiency for tarantula (*E. californicum*) Hc-d PO to be 3.91 $\text{mM}^{-1} \text{S}^{-1}$ for dopamine and 0.59 for L-DOPA. Our kinetic data for the Hc-dopamine complex ($V_{max} = \sim 4.9$ $\mu\text{mol min}^{-1}$; $K_M = \sim 0.8$ mM) are in good agreement with those published by Wright *et al.* (2012) for *L. polyphemus*; $V_{max} = 4.8$ $\mu\text{mol min}^{-1}$, $K_M = 1.1$ mM. Collectively, these data support the use of dopamine as a positive control for characterising Hc-d PO activity.

3.2 Antibacterial and antifungal assays

Using both endogenous and synthetic substrates (dopamine, L-DOPA, 4-MC, 4-TBC) at a standardised concentration of 2 mM, we tested the antimicrobial potential of the respective *ortho*-quinone derivatives (dopaminechrome, dopachrome, 4-methyl-o-benzoquinone; 4-*tert*-butyl-o-benzoquinone). Generally, the exposure of bacteria and yeast to the products of Hc-d PO activity (using each substrate) led to significant reductions in colony forming units (CFUs), $F_{(4,60)} = 211.6$, $P < 0.0001$ (Figure 2). Treating microbes for one hour was sufficient time for the Hc-produced *o*-quinones to inflict damage or hinder replication. Microbicidal potency ranged from 28.7 – 81% for L-DOPA, 59.3 – 89.3% for dopamine, 67 – 83.9% for 4-MC, and 69 – 94.7% for 4-TBC. Taking a closer look at the antibacterial effects, Gram-negative bacteria were highly susceptible to all the reaction products generated (Figure 2), whereas Gram-positive bacteria were more resilient to L-DOPA. This observation is similar to one made by Cerenius *et al.* (2010); despite using alternative microbes to us (see Table 2), Gram-negative bacteria were markedly more sensitive to the reactions products of crayfish PO. CFU numbers in the presence of dopamine, 4-MC and 4-TBC

different to the control and 4-TBC values ($P = 0.005$ and 0.0023 , respectively). With the exception of *B. megaterium*, 4-TBC was demonstrably the most effective at prohibiting microbial growth (Figure 2).

4. Discussion

Mollusc and arthropod hemocyanins (Hcs) contribute in many ways to immune defences, such as the inhibition of viral replication, the liberation of AMPs, and the conformational switch to a PO-like enzyme (reviewed by Coates and Nairn, 2014). Reaction products from crustacean (Cerenius et al. 2010; Charoensapsri et al., 2014), insect (Zhao et al., 2007) and bivalve (Xing et al., 2012) POs in the presence of dopamine and/or L-DOPA can agglutinate and kill microbes, including the vertebrate pathogens *Candida albicans* and *Vibrio parahaemolyticus* (Table 2). Such reactive by-products tend to be oxidising (e.g. O_2^-) and nitrosative (e.g. $ONOO^-$) species, alongside semi-quinone intermediates. These compounds can also cause harm to the host so they must be regulated carefully (reviewed by Cerenius et al., 2008).

Often, it is assumed that the by-products of Hc-d PO activity are antagonistic toward pathogens – yet until now, evidence has been lacking. We close this knowledge gap by presenting data that clearly links catalytic efficacy of activated Hc to the antimicrobial capacity of its substrates/products (Table 1; Figure 2). The three following details prove that diminished CFU numbers are due to the toxicity of Hc-d PO reaction products. (1) When Hc was exposed to the PO-specific inhibitor, phenylthiourea, enzymatic activity was disrupted and CFU numbers remained consistent with the controls, >98%. (2) Each of the assay mixtures failed to kill microbes when Hc was omitted entirely. (3) As arthropod Hc oligomers (hexamers ~420 kDa) and individual subunits (~70 kDa) are known to inflict damage upon binding directly to bacteria and viruses (Coates and Decker, 2017), we used a >10 kDa filter to remove Hc from the reaction mixtures prior to microbial exposure. Earlier observations by Jiang et al. (2007) complement our study. Hc from the mangrove horseshoe crab (*Carcinoscorpius rotundicauda*) displayed antiseptic properties when incubated with the protease-secreting bacterium *Pseudomonas aeruginosa* and the substrate 4-MC *in vitro* (Jiang et al., 2007). In a second experiment, the authors injected *C. rotundicauda* with 1×10^5 CFUs of *Staphylococcus aureus* in the absence and presence of the PO inhibitor kojic acid. The hemolymph of animals treated with kojic acid contained significantly higher bacterial loads, suggesting the inhibition of Hc-d PO activity compromised the host's defences.

The conversion of arthropod Hc into Hc-d PO involves the relocation, or complete removal, of the N-terminal domain away from the central domain where the dicopper active site is located (Baird et al., 2007). These structural rearrangements open-up a channel for bulky phenolic compounds to enter the active site and undergo oxidation.

cuticle during wound repair then Hc may utilise similar compounds with catechol moieties or intermediate substrates of the melanogenesis pathway, including 5,6-Dihydroxyindole (DHI; Adachi *et al.*, 2005). We encountered solubility issues when handling DHI, however like Adachi *et al.* (2005), we did observe a noticeable increase in DHI oxidation in the presence of activated *L. polyphemus* Hc (data not shown). Interestingly, DHI is an effective biocide against viruses (λ -bacteriophage) and parasites of insects (*Microplitis demolitor* Zhao *et al.*, 2011), and crayfish (*Aphanomyces spp.*; Söderhäll and Ajaxon, 1982). The ability of chelicerate Hcs to catalyse substrates downstream of L -tyrosine/ L -DOPA (e.g. DHI, *N*-acetyldopamine and epinephrine; Decker and Jaenicke, 2008), the association of Hc with clot formation in spiders (Sanggaard *et al.*, 2016), and the activation of horseshoe crab Hc by clotting factors and chitin-binding AMPs (Nagai and Kawabata, 2000; Nagai *et al.*, 2001), all infer a role for Hc in both the sclerotinogenic and melanogenic pathways.

We documented arthropod Hc accommodating various diphenolic substrates into the dicopper active site and converting them into antimicrobial (highly reactive) products in a similar manner to true PO enzymes (tyrosinase [EC 1.14.18.1] and catecholoxidase [EC 1.10.3.1]). After careful consideration of the available literature and evaluation of our results, we form the opinion that Hc is an integral component of invertebrate anti-infective responses.

Acknowledgements

This study was financed by start-up funds (College of Science, Swansea University) assigned to C.J.C.

Author contributions

C.J.C conceived and designed the experiments. C.J.C. and J.T. performed the experiments and analysed the data. C.J.C. collated information and wrote the manuscript.

References

- Adachi, K., Wakamatsu, K., Ito, S., Miyamoto, N., Kokubo, T., Nishioka, T., & Hirata, T. (2005). An oxygen transporter hemocyanin can act on the late pathway of melanin synthesis. *Pigment Cell & Melanoma Research*, 18(3), 214-219.
- Baird, S., Kelly, S. M., Price, N. C., Jaenicke, E., Meesters, C., Nillius, D., Decker, H., & Nairn, J. (2007). Hemocyanin conformational changes associated with SDS-induced phenol oxidase activation. *Biochimica et Biophysica Acta (BBA)-Proteins and Proteomics*, 1774(11), 1380-1394.

Coates, C. J., Whalley, T., Wyman, M., & Nairn, J. (2013). A putative link between phagocytosis-induced apoptosis and hemocyanin-derived phenoloxidase activation. *Apoptosis*, 18(11), 1319-1331.

Cerenius, L., Babu, R., Söderhäll, K., & Jiravanichpaisal, P. (2010). *In vitro* effects on bacterial growth of phenoloxidase reaction products. *Journal of invertebrate pathology*, 103(1), 21-23.

Cerenius, L., Lee, B. L., & Söderhäll, K. (2008). The proPO-system: pros and cons for its role in invertebrate immunity. *Trends in immunology*, 29(6), 263-271.

Charoensapsri, W., Amparyup, P., Suriyachan, C., & Tassanakajon, A. (2014). Melanization reaction products of shrimp display antimicrobial properties against their major bacterial and fungal pathogens. *Developmental & Comparative Immunology*, 47(1), 150-159.

Dolashka, P., Dolashki, A., Beeumen, J. V., Floetenmeyer, M., Velkova, L., Stevanovic, S., & Voelter, W. (2016). Antimicrobial activity of molluscan hemocyanins from *Helix* and *Rapana* snails. *Current pharmaceutical biotechnology*, 17(3), 263-270.

Jaenicke, E., & Decker, H. (2008). Kinetic properties of catecholoxidase activity of tarantula hemocyanin. *The FEBS journal*, 275(7), 1518-1528.

Jiang, N., Tan, N. S., Ho, B., & Ding, J. L. (2007). Respiratory protein-generated reactive oxygen species as an antimicrobial strategy. *Nature immunology*, 8(10), 1114.

Jiang, J., Zhou, Z., Dong, Y., Cong, C., Guan, X., Wang, B., et al., (2014). *In vitro* antibacterial analysis of phenoloxidase reaction products from the sea cucumber *Apostichopus japonicus*. *Fish & shellfish immunology*, 39(2), 458-463.

Lee, S. Y., Lee, B. L., & Söderhäll, K. (2003). Processing of an antibacterial peptide from hemocyanin of the freshwater crayfish *Pacifastacus leniusculus*. *Journal of Biological Chemistry*, 278(10), 7927-7933.

Nagai, T., & Kawabata, S. I. (2000). A link between blood coagulation and prophenol oxidase activation in arthropod host defense. *Journal of Biological Chemistry*, 275(38), 29264-29267.

Nagai, T., Osaki, T., & Kawabata, S. I. (2001). Functional conversion of hemocyanin to phenoloxidase by horseshoe crab antimicrobial peptides. *Journal of Biological Chemistry*, 276(29), 27166-27170.

Sanggaard, K. W., Dylund, T. F., Bechsgaard, J. S., Scavenius, C., Wang, T., Bilde, T., & Enghild, J. J. (2016). The spider hemolymph clot proteome reveals high concentrations of hemocyanin and von Willebrand factor-like proteins. *Biochimica et Biophysica Acta (BBA)-Proteins and Proteomics*, 1864(2), 233-241.

Schenk, S., Schmidt, J., Hoeger, U., & Decker, H. (2015). Lipoprotein-induced phenoloxidase-activity in tarantula hemocyanin. *Biochimica et Biophysica Acta (BBA)-Proteins and Proteomics*, 1854(8), 939-949.

Söderhäll, K., Ajaxon, R. (1982). Effect of quinones and melanin on mycelial growth of *Aphanomyces* spp. and extracellular protease of *Aphanomyces astaci*, a parasite on crayfish. *Journal of invertebrate pathology*, 39(1), 105-109.

Whitten, M., & Coates, C. J. (2017). Re-evaluation of insect melanogenesis research: Views from the dark side. *Pigment cell & melanoma research*.

Wright, J., Clark, W. M., Cain, J. A., Patterson, A., Coates, C. J., & Nairn, J. (2012). Effects of known phenoloxidase inhibitors on hemocyanin-derived phenoloxidase from *Limulus polyphemus*. *Comparative Biochemistry and Physiology Part B: Biochemistry and Molecular Biology*, 163(3-4), 303-308.

Xing, J., Jiang, J., & Zhan, W. (2012). Phenoloxidase in the scallop *Chlamys farreri*: purification and antibacterial activity of its reaction products generated *in vitro*. *Fish & shellfish immunology*, 32(1), 89-93.

Zhao, P., Li, J., Wang, Y., & Jiang, H. (2007). Broad-spectrum antimicrobial activity of the reactive compounds generated *in vitro* by *Manduca sexta* phenoloxidase. *Insect biochemistry and molecular biology*, 37(9), 952-959.

Table 1 Kinetic properties of hemocyanin-derived phenoloxidase activity

Substrate	V_{max} [$\mu\text{mol min}^{-1}$]	K_M [mM]	K_{cat}/K_M [$\text{mM}^{-1} \text{S}^{-1}$]
Caffeic acid ^a	1.98 ± 0.079	4.76 ± 0.433	0.51 ± 0.02
Catechol	1.82 ± 0.132	7.02 ± 0.786	0.32 ± 0.02
Dopamine	4.86 ± 0.099	0.79 ± 0.053	4.43 ± 0.09
L-DOPA ^b	1.52 ± 0.097	1.87 ± 0.283	0.58 ± 0.037
DOPAC ^c	1.28 ± 0.095	12.97 ± 0.609	0.12 ± 0.009
4-Methylcatechol	7.36 ± 0.196	1.67 ± 0.194	3.2 ± 0.085
4- <i>tert</i> -Butylcatechol	9.27 ± 0.37	1.17 ± 0.11	5.71 ± 0.22

^a3,4-Dihydroxycinnamic acid

^b3,4-Dihydroxyphenylalanine

^c3,4-Dihydroxyphenylacetic

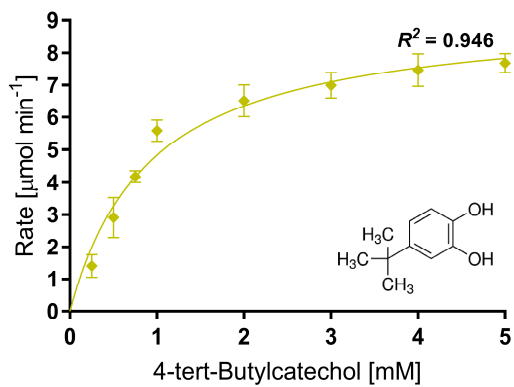
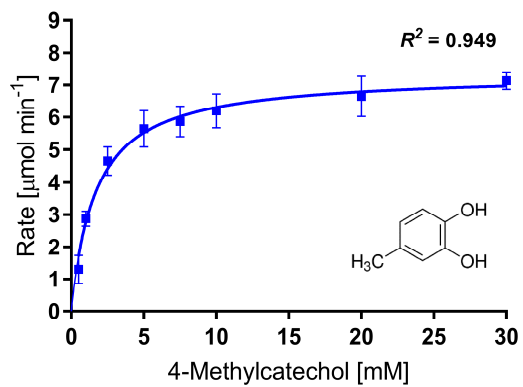
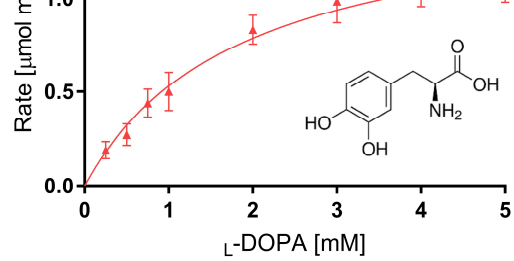
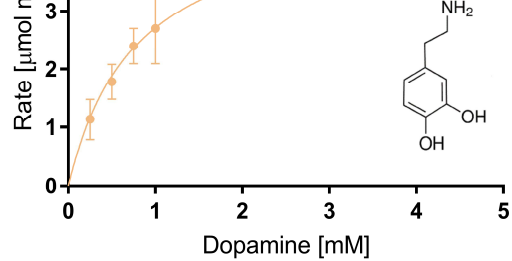
acid.

Table 2 Broad spectrum antimicrobial activities of phenoloxidase-like enzyme reaction products

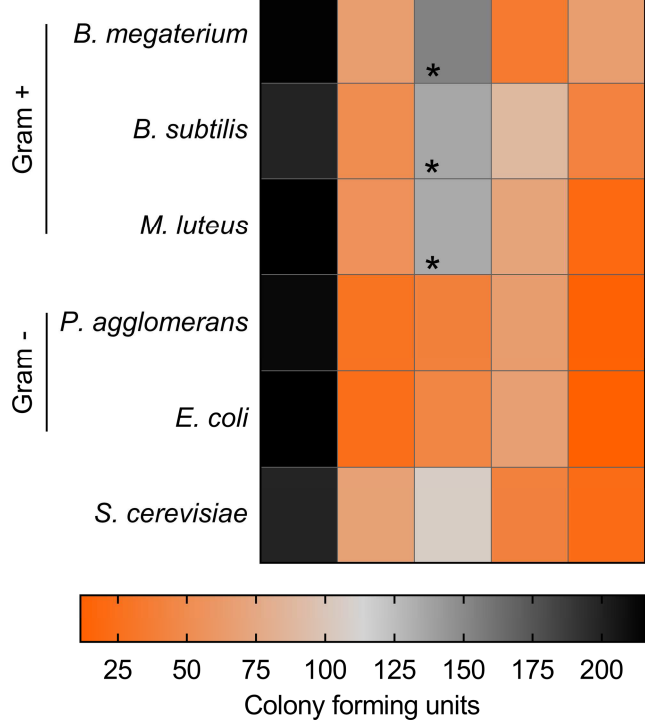
Species	Substrates (diphenols)	Anti-infective activity (targets)
<i>Apostichopus japonicus</i> [sea cucumber PO]	L-DOPA; dopamine	Antibacterial (Gram +/-) <i>Vibrio splendidus</i> ; <i>V. harveyi</i> ; <i>Staphylococcus aureus</i> [cell lysis]
<i>Carcinoscorpius rotundicauda</i> [horseshoe crab Hc]	4-Methylcatechol	Antibacterial (Gram -) <i>Pseudomonas aeruginosa</i>
<i>Chlamys farreri</i> [scallop PO]	L-DOPA; dopamine	Antibacterial (Gram +) <i>Vibrio alginolyticus</i> ; <i>V. parahaemolyticus</i> ; <i>Aeromonas salmonicida</i> [agglutination]
<i>Limulus polyphemus</i> [horseshoe crab Hc]	L-DOPA; dopamine; 4-MC; 4-TBC;	Antimicrobial (Gram +/- bacteria, fungi) <i>Bacillus megaterium</i> ; <i>Bacillus subtilis</i> ; <i>Saccharomyces cerevisiae</i> ; <i>Escherichia coli</i> ; <i>Micrococcus luteus</i> ; <i>Pantoea agglomerans</i> ; <i>Erwinia herbicola</i>
<i>Manduca sexta</i> [insect PO]	L-DOPA; dopamine; DHI; NADA	Antimicrobial (Gram +/- bacteria, fungi) <i>Escherichia coli</i> ; <i>Klebsiella pneumoniae</i> ; <i>Pseudomonas aeruginosa</i> ; <i>Salmonella typhimurium</i> ; <i>Bacillus subtilis</i> ; <i>B. cereus</i> ; <i>Micrococcus luteus</i> ; <i>Staphylococcus aureus</i> ; <i>Pichia pastoris</i> ; <i>Saccharomyces cerevisiae</i> ; <i>Beauveria bassiana</i> ; [cell agglutination]
<i>Pacifastacus leniusculus</i> [crayfish PO]	L-DOPA; dopamine	Antibacterial (Gram +/-) <i>Aeromonas hydrophila</i> ; <i>Escherichia coli</i> ; <i>Streptococcus pneumoniae</i> ; <i>Saccharomyces cerevisiae</i> ; <i>Pseudomonas aeruginosa</i> ; <i>Staphylococcus aureus</i>
<i>Penaeus monodon</i> [shrimp PO]	L-DOPA; dopamine; DHI	Antibacterial (Gram +/-) <i>Vibrio harveyi</i> ; <i>Vibrio parahaemolyticus</i> ; <i>Bacillus subtilis</i> ; <i>Flavobacterium columnare</i> [membrane damage]
5,6-dihydroxyindole [DHI]; 3,4-dihydroxy-L-phenylalanine	[L-DOPA]; N-acetyldopamine [NADA]; hemocyanin	

Figure 1 Hemocyanin-derived phenoloxidase activity in the presence of various diphenolic substrates *in vitro*. Hemocyanin (1 mgmL⁻¹) purified from *Limulus polyphemus* was activated with SDS (0.1%) for 5 minutes prior to the addition of each substrate. Product accumulation was monitored at 475 nm (indicative of quinone formation) for 5 minutes. Enzyme-substrate interactions were analysed using Michaelis-Menten kinetics (non-linear regression) in GraphPad PRISM v7. Values represent mean ± standard deviation (*n* = 3). Chemical structures for each diphenol are presented.

Figure 2 Effect of hemocyanin-derived phenoloxidase reaction products on microbes *in vitro*. Hemocyanin (1 mgmL⁻¹) purified from *Limulus polyphemus* was activated with SDS (0.1%) for 5 minutes prior to the addition of each diphenolic substrate. After 5 minutes, hemocyanin was filtered (>10 kDa cut-off) using centrifugation and the reaction mixtures were exposed to Gram-positive bacteria (*B. megaterium*, *B. subtilis*, *M. luteus*), Gram-negative bacteria (*E. coli*, *P. agglomerans*) and/or yeast (*S. cerevisiae*). The heat map displays mean colony forming units of treated microbes (*n* = 3). The asterisk represents significant differences between L-DOPA and each of the remaining substrates in that row, i.e., dopamine, 4-Methylcatechol and 4-*tert*-Butylcatechol.



ACCEPTED MANUSCRIPT



ACCEPTED MANUSCRIPT

ACCEPTED MANUSCRIPT

- Chelicerate hemocyanin is a contributing factor to melanogenesis
- Hemocyanin catalytic efficiency correlates broadly with antimicrobial potential
- Horseshoe crab hemocyanin is an integral component of innate immunity

ACCEPTED MANUSCRIPT